Recycling and evaluation of poly(ethylene terephthalate) waste as effective corrosion inhibitors for C-steel material in acidic media

3 authors, including:

Moayad N. Khalaf
University of Basrah
108 PUBLICATIONS   **142** CITATIONS

Int. J. Corros. Scale Inhib., 2020, **9**, no. 2, 427–445

427

Recycling and evaluation of poly(ethylene terephthalate) waste as effective corrosion inhibitors for C-steel material in acidic media

R.J. Tuama,[1] M.E. Al-Dokheily[2]* and M.N. Khalaf[3]

[1]Department of Pharmacognosy, College of Pharmacy, ThiQar University, Iraq
[2]Department of Chemistry, College of Science, ThiQar University, Iraq
[3]Department of Chemistry, College of Science, Basrah University, Iraq
E-mail: mohsin552015@gmail.com

Abstract

Depolymerization of waste polyethylene terephthalate (PET) was achieved by propane-1,3-dithiol into bis(3-mercaptopropyl)thioterephthalate (BTPTT) product. The product was characterized by FTIR and GPC. The thermal properties (TGA, DTA) indicated that the prepared compound was thermally stable up to 150°C. The corrosion inhibition efficiency of the new compound as a corrosion inhibitor was evaluated for carbon steel in 0.1 N HCl as a corrosive environment and the inhibitor concentration was (0, 5, 10, 15, 20 and 25 ppm). The inhibition efficiency was measured by using Tafel plot in electrochemical technique. The results indicated that the effectiveness of the bis(3-mercaptopropyl)thioterephthalate as an inhibitor increases with the concentration but this characteristic is inversely related to the temperature. The inhibition efficiency (%*IE*) reached 97.32% for the 25 ppm concentration at 298 K. Potentiodynamic polarization measurements revealed that the product is a corrosion inhibitor of anodic type. The results showed that the inhibition occurs through adsorption of the inhibitor molecules on the C-steel surface. The adsorption of (BTPTT) on C-steel surface obeys the Langmuir adsorption isotherm and involves a chemisorption mechanism.

1. Introduction

Recycling is described as the way toward recouping scrap or waste plastic and reprocessing the material into useful items. Since the majority of plastic is non-biodegradable, in particular poly (ethylene terephthalate), recycling of PET has become a significant procedure from the environmental point of view and it has given commercial opportunity because of wide spread use and availability of PET bottles, packages and fiber [1, 2]. Recycling processes are the best way to economically reduce PET waste and these processes must be established for the preservation of resources and the protection of the global environment [3–5].

Corrosion is one of the most important industrial problems facing the developed world, causing corrosion annually to close many of factories and stop installations, loss of many industrial products, leading to damage them eventually involve pollution of the environment [6–8]. Corrosion is a chemical or electrochemical oxidation process, in which the metal exchange electrons to the environment and undergo a valance change from zero to a positive value [9, 10]. In most industrial fields, corrosion cannot be completely prevented or reduced, but there are many methods that could be used to minimize or control corrosion with insignificant losses and costs. Corrosion control is accomplished by perceiving and understanding corrosion mechanisms, using corrosion-resistant materials and modifying designs, additionally by using protective systems, devices, and treatments [11–13]. Utilization of chemical inhibitors is one of the most successful ways to avoid deterioration of materials. The organic compounds including of N, S, and O heteroatoms as well as pi-electron systems were commonly employed as inhibitors to protect metals from corrosion in many aggressive acidic media. The efficiency of these compounds mainly relies upon their abilities to be adsorbed on the metal surface with the polar groups going about as reactive centers [14–17]. Therefore the impact of temperature on the inhibited acid-metal reaction is highly complex. So, this research facilitates the determination of many thermodynamic functions for the inhibition and/or the adsorption processes which contribute in deciding the adsorption type of inhibitors.

The aim of this paper is to research waste PET-bottle depolymerization by propane-1,3-dithiol to produce bis(3-mercaptopropyl)thioterephthalate, the product was tested as a corrosion inhibitor for carbon steel in 0.1 N HCl.

2. Experimental

2.1. Materials

A carbon steel (C1010) acquired from Metal Samples (USA). It has the following compositions by percentage weight: C = 0.13%, Mn = 0.3%, Si = 0.37%, P = 0.04%, S = 0.05%, Cr = 0.1%, Ni = 0.3%, Cu = 0.3%, As = 0.08% and the residue is Fe. Poly (ethylene terephthalate) (PET) waste was beverage bottle. Propane-1,3-dithiol, zinc acetate and HCl were acquired from Sigma-Aldrich Chemical Co.

2.2. Instruments

Bruker-Vertex FTIR spectrophotometer was utilized for revelation of chemical structure through the Fourier transform infrared spectral data in 400–4000 cm^{-1} wavenumber range. The molar weights and other related properties of prepared sample was analyzed by gel permeation chromatography (GPC) with refractive index detector using Breeze™ 2 HPLC System, THF (Merck) was used as the eluent at a flow rate of 1.0 ml/min. BAHR-Thermo analyser (STA 503) was used for the thermal analysis study (TGA&DTA). The rate of heating was 20°C/min in an inert atmosphere of argon.

2.3. Recycling process

PET bottles, after removing caps and labels, were washed, dried and cut into small chips with a diameter of (3–6) mm. PET chips were depolymerized with propan-1,3-dithiol, at weight ratio of PET to propan-1,3-thiol 1:6 (wt% of PET: wt% of propan-1,3-dithiol) in the presence of the catalyst 1% zinc acetate (by weight based on weight of PET). This reaction was carried out in 250 mL round bottomed flask with a thermometer and are flux condenser. The reaction mixture were heated under vigorous stirring in nitrogen atmosphere at a temperature about (160–180)°C for 8 h then at 140°C for 2 h. The mixture was permitted to cool to room temperature. Toward the finish of the response, distilled water was added in abundance to the reaction mixture with vigorous agitation and heating. Then, this mixture was separated. The collected filtrate was stocked in a fridge at 0°C for 24 h. White crystalline flakes were formed in the filtrate indicating precipitation of an oligomer bis(3-mercaptopropyl)thioterephthalate (BTPTT) out of the product, and it was separated and dried [18, 19]. The suggested mechanism was shown in (Scheme 1).
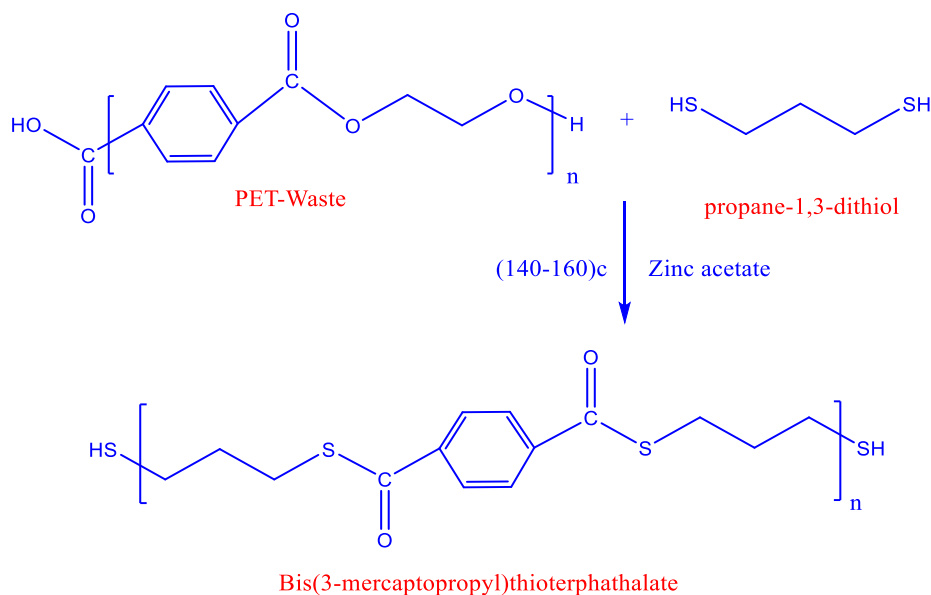
Scheme 1. Mechanism for the preparation of (BTPTT).

2.4. Preparation of the carbon steel plates

The corroded (WE) was polished with carbide sheets having the range from 600 to 1200 grade. A carbon steel plate was then rinsed with distilled water, acetone, and ethanol several times. It was then immediately dried in a furnace for 15 min at 40°C.

2.5. Electrochemical measurements

A carbon steel examined as metal sample immersed in acidic solution contains 0.1 N hydrochloric acid (HCl) with various concentrations (0, 5, 10, 15, 20 and 25 ppm) of

bis(3-mercaptopropyl)thioterephthalate (BTPTT) as corrosion inhibitor at various temperatures (298–328 K). The electrochemical measurements were performed using a DY 2300 Series Potentiostat/Bipotentiostat fully computerized in the processed data analysis. A three-electrode cell assembly, consisting of C-steel as the working electrode (WE), platinum as the counter electrode (CE) and a silver–silver chloride electrode as the reference electrode (RE). Water bath used to control the temperature of the electrolyte during running of the test. The data of electrochemical measurements started after one hour from immersing the working electrode (WE) in the test solution at open circuit potential, that is the time to allow a steady state potential to stabilize. From the polarization information, numerous parameters were determined like the percentage inhibition efficiency (%*IE*), the degree of surface coverage (θ), corrosion rate (*CR*) and charge transfer resistance (R_{ct}) [20, 21].

The inhibition efficiency (%*IE*) was calculated according to equation (1), while the surface coverage (θ) value was determined using equation (2). Where $CR_{(uninhib)}$ and $CR_{(inhib)}$ were the values of the corrosion rate of C-steel without and with inhibitor presence respectively [22, 23].

$$\% IE = \frac{CR_{(uninhib)} - CR_{(inhib)}}{CR_{(uninhib)}} \times 100 \tag{1}$$

$$\theta = \frac{CR_{(uninhib)} - CR_{(inhib)}}{CR_{(uninhib)}} \times 100 \tag{2}$$

2.6 Adsorption isotherm

Adsorption isotherms were employed to comprehend the connection between the inhibitor (adsorbate) and an adsorbent surface [24]. It is a general supposition that, the adsorption of the organic inhibitors at the metal interface is the initial step in the system of inhibitors activity. The adsorption process comprises of the substitution of water molecules at a corroding interface as indicated by following procedure [25].

$$\text{Org}_{(sol)} + n\text{H}_2\text{O}_{(ads)} \leftrightarrow \text{Org}_{(ads)} + n\text{H}_2\text{O}_{(sol)} \tag{3}$$

where $\text{Org}_{(sol)}$ and $\text{Org}_{(ads)}$ are the organic molecules in the solution and adsorbed on the metal surface, respectively, and *n* is the number of water molecules supplanted by the organic molecules. Organic molecules may adsorb on the metal surface in four types [26]:

    i) Electrostatic interaction between the charged particles and the charged metal surface.
    ii) Interaction of uncharged electron pairs in the particles and metal.
    iii) Interaction of π-electrons with metal.
    iv) A mix of the types (i) and (iii).

In general, two models of adsorption can be considered. The procedure of physical adsorption requires presence of electrically charged metal surface and charged species in the greater part of solution. Chemisorption process includes charge sharing or charge transfer from the inhibitor molecules to the metal surface. The most likely mechanism by which organic compounds inhibit metal corrosion is the adsorption organic molecules on the metallic surface. Adsorption isotherms can provide significant data about the nature of interactions that exist at the metal/solution interface where both the water and inhibitor molecules are available [27, 28]. Langmuir, Freundlich and Temkin were employed to establish the isotherms most appropriate to experimental data.

2.7. Characterization for inhibitor

Figure 1 shows the FTIR spectra of bis(3-mercaptopropyl)thioterephthalate (BTPTT). An absorption peak at (3078.39) cm^{-1} is attributable to aromatic stretching of (−CH) group, while the peaks spotted at (817.82) and (756.10) cm^{-1} refer to olefinic and aromatic (−CH) out of plane bending of para-substituted phenyl.

The stretching mode of (S−H) group is confirmed by a weak peak present at the wavenumbers of (2360.87) cm^{-1}. The peak at (1689.64) cm^{-1} is ascribed to the stretching vibration of the (C=O) group and the peak at (1234.44) cm^{-1} is attributable to the (C−O) bond, while the peaks at (1566.20) cm^{-1} and (1427.32) cm^{-1} correspond to aromatic stretching of the (C=C) group.

Figure 2 shows the GPC of bis(3-mercaptopropyl)thioterephthalate (BTPTT), the molecular weights of (BTPTT) and polydispersity index were determined by using GPC technique. The number-average molecular weight (*Mn*) and the weight-average molecular weight (*Mw*) of (BTPTT) were found at (1080.5) g/mol and (1576.8) g/mol respectively, while the peak molecular weight of (BTPTT) was found at (919.46) g/mol. The value of polydispersity index (*Mw*/*Mn*) for (BTPTT) was equal to (1.459).
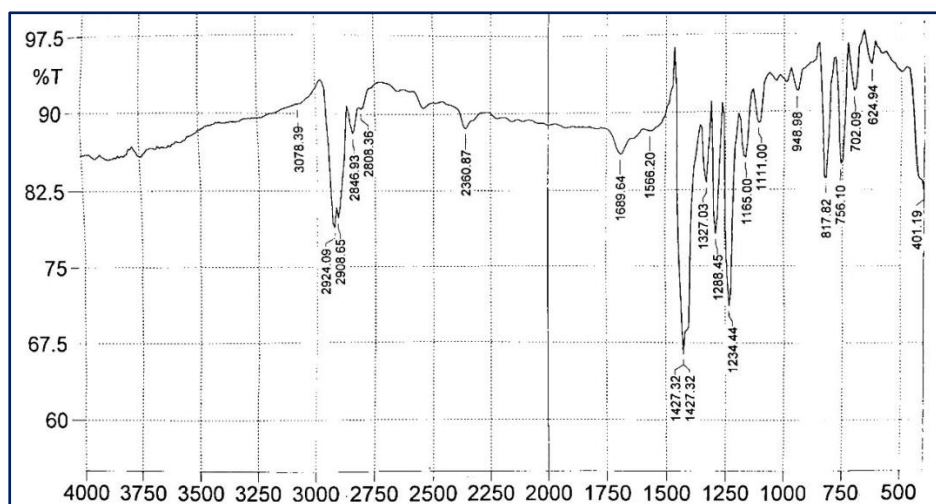

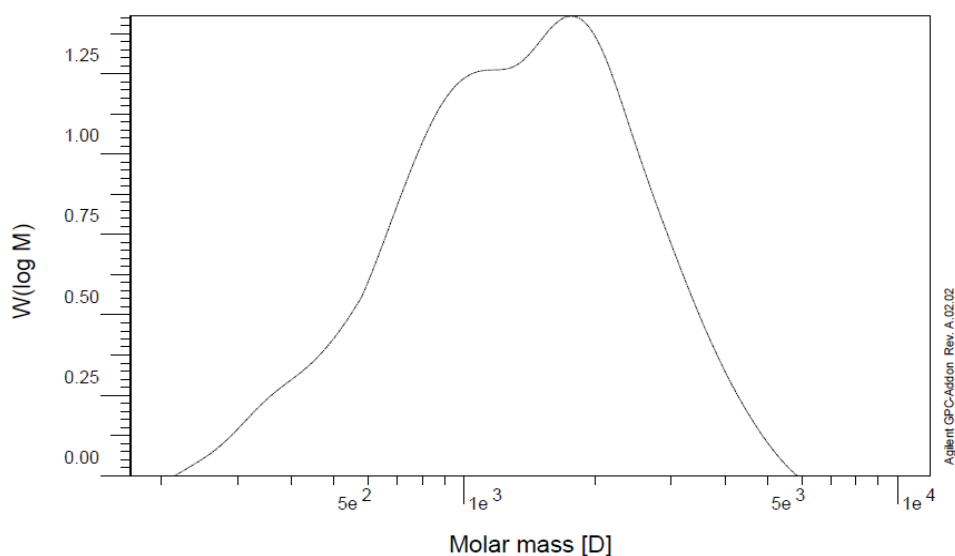**Figure 1.** FTIR spectrum of compound (BTPTT).

Figure 2. GPC chromatograms of compound (BTPTT).

3. Results and discussion

3.1. Electrochemical measurements

3.1.1. Potentiodynamic polarization measurements (Tafel method)

The potentiodynamic polarization measurement results for C-steel in 0.1 N HCl in the presence and absence of inhibitor concentration of (BTPTT) at various temperatures (298–328) K are shown in the related Tafel curves (Figures 3–5). The polarization parameters, namely corrosion current density (I_{corr}), corrosion potential (E_{corr}), corrosion rate, charge transfer resistance (R_{ct}), percentage inhibition efficiency (%IE), and surface coverage (θ) are given in Table 1.

Table 1. Tafel parameters for C-steel in 0.1 N HCl in the absence and presence of different concentrations of BTPTT at different temperatures.

Conc. ppm	T K	E_{corr} mV	I_{corr} µA/cm²	R_{ct} Ω	CR mpy	%IE	θ
Blank		−617	1056	12.2	116	–	–
5		−483	72.864	176.81	8	93.1	0.931
10	298	−480	62.304	206.77	6.8	94.1	0.941
15		−482	57.024	225.92	6.23	94.6	0.946
20		−484	46.464	277.27	5.1	95.6	0.956
25		−490	28.3008	455.22	3.21	97.32	0.9732

Conc. ppm	T K	E_{corr} mV	I_{corr} $\mu A/cm^2$	R_{ct} Ω	CR mpy	%IE	θ
Blank		−611	1120	10.15	128	–	
5		−615	89.264	127.35	10.2	92.03	0.9203
10	308	−500	84	135.3	9.5	92.5	0.925
15		−450	71.68	158.5	8.1	93.6	0.936
20		−510	55.216	205.88	6.03	95.07	0.9507
25		−500	42	270.6	4.8	96.25	0.9625
Blank		−625	1304	8.95	183.6	–	
5		−560	108.232	107.83	15.2	91.7	0.917
10	318	−528	100.408	116.23	14.06	92.3	0.923
15		−516	89.976	129.71	12.53	93.1	0.931
20		−502	78.3704	148.91	11.03	93.99	0.9399
25		−503	67.808	172.11	9.4	94.8	0.948
Blank		−628	1430	7.433	259	–	
5		−630	227.513	46.71	41.2	84.09	0.8409
10	328	−625	215.93	49.2	39	84.9	0.849
15		−620	199.914	53.16	36.2	86.02	0.8602
20		−626	177.32	59.94	31.9	87.6	0.876
25		−621	151.58	70.12	27.4	89.4	0.894

The data clearly indicate that the (I_{corr}) values decreased and (R_{ct}) values increased in the presence of the inhibitor at various concentrations as expected. Referable to the inverse relationship between (I_{corr}) and (R_{ct}), with increasing concentration of the inhibitor, it can be taken for granted that the adsorption of the inhibitor molecules on metal surface makes a physical barrier to the mass and charge transfer, giving a high level of protection to the metal surface by hindering the active sites on the metal [26, 29]. In literature, an inhibitor can be named cathodic or anodic type if the move of corrosion potential (E_{corr}) brought about by the inhibitor is higher than 85 mV and as mixed type if the displacement of corrosion potential lower than 85 mV [30–32]. It was found that the values of E_{corr} are shifted toward the positive direction by increasing the concentrations of inhibitor (BTPTT). The maximum shift in the E_{corr} with addition of inhibitor was 127 mV at 298 K, which suggests anodic type inhibitor behavior for the different concentrations studied [33, 34].
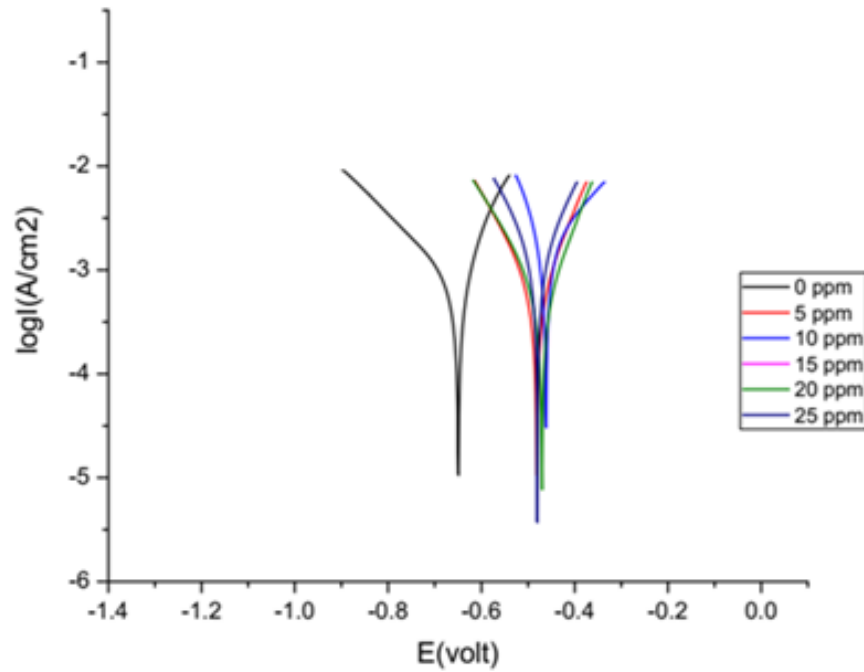
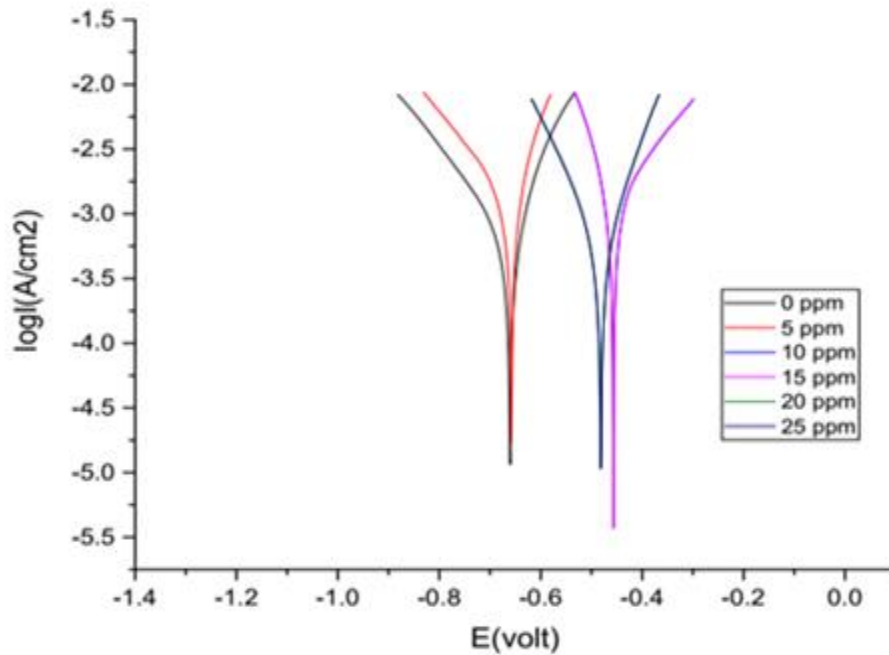**Figure 3.** Tafel plots for C-steel in 0.1 N HCl without and with various concentrations of BTPTT inhibitor at 298 K.

Figure 4. Tafel plots for C-steel in 0.1 N HClwithout and with various concentrations of BTPTT inhibitor at 308 K.
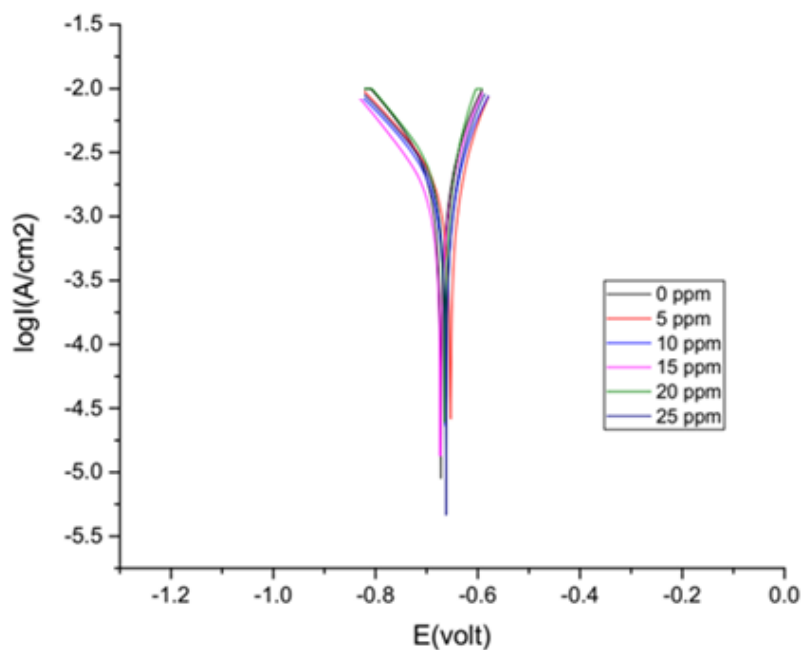
Figure 5. Tafel plots for C-steel in 0.1 N HCl without and with various concentrations of BTPTT inhibitor at 328 K.

The values of the (θ) and (%*IE*) reached its maximum at (BTPTT) concentration of 25 ppm at 298 K. From the results the inhibition efficiencies increased with increasing of inhibitor concentration and this could have been explained on the basis of the amount of adsorption with inhibitor coverage molecules, increases with increasing concentrations. The inhibition performance increased in parallel with concentration of inhibitor increased, that suggests the retardation of surface of C-steel corrosion in inhibited solution compared to uninhibited environment [33].
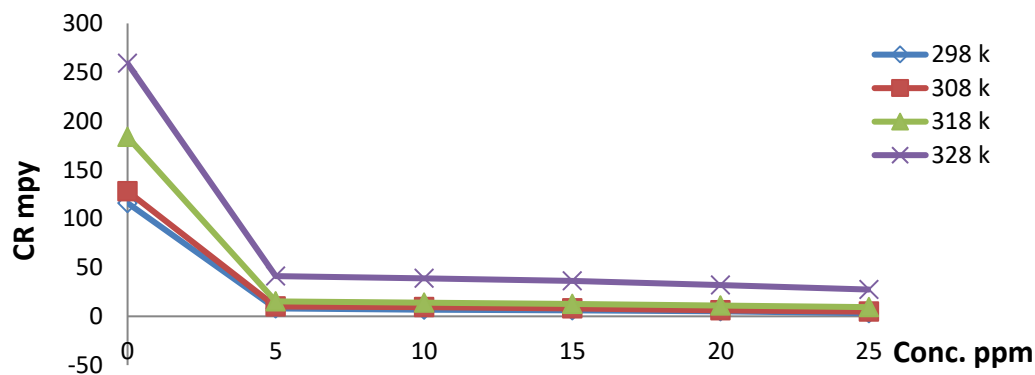

Figure 6. Effect of inhibitor concentration on corrosion rate of C-steel in0.1 N HCl at different temp.
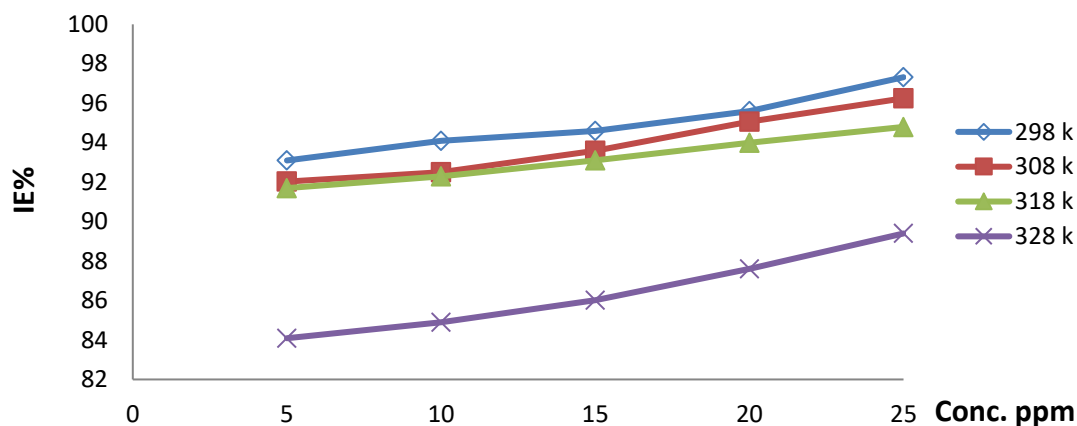
Figure 7. Effect of inhibitor concentration on *IE*% of inhibitor at different temp.

3.1.2. Effect of temperature

It is considered the effect of temperature on the inhibited acid–metal reaction is highly complex, because many changes occur on the metal surface such as adsorption, desorption, rearrangement or decomposition of the inhibitor [35]. This was accomplished by examining the temperature dependence of the corrosion current, exploring the activation energy of the corrosion process and the thermodynamic functions of adsorption of inhibitor (BTPTT). The influence of increasing temperature from (298–328) K on the corrosion rate of C-steel in 0.1 N HCl, and its effects on inhibition action of 25 ppm (BTPTT) are appeared in Table 2. It is commented that the corrosion rate in acid solutions increases with increasing temperature, while the inhibition efficiency decreases with increasing temperature.

At concentration 25 ppm, the inhibitory effect (%*IE*) decreased from 97.32% at 298 K to 89.4% at 328 K indicating that higher temperature dissolution of the C-steel predominates on adsorption of (BTPTT) molecules at C-steel surface.

Table 2. The effect of temperature on the corrosion rates of C-steel in the absence and presence of 25 ppm of BTPTT inhibitor.

T (K)	0.1 N HCl *CR* (mpy)	BTPTT *CR* (mpy)	%*IE*	θ
298	116	3.21	97.32	0.973
308	128	4.8	96.25	0.962
318	183.6	9.4	94.8	0.948
328	259	27.4	89.4	0.894

The activation parameters for the corrosion process such as activation energy E_a^*, activated entropy ΔS_a^* and activated enthalpy ΔH_a^* were calculated from Arrhenius equation and its alternative formulation called transition state equation according to the following equations [36]:

$$CR = A\exp\left(-\frac{E_a}{RT}\right) \tag{4}$$

$$CR = \frac{RT}{Nh}\exp\left(\frac{\Delta S_a}{R}\right)\exp\left(-\frac{\Delta H_a}{RT}\right) \tag{5}$$

where CR is the corrosion rate, A the pre-exponential factor, E_a^* is the apparent activation energy, h is the Planck's constant 6.626176×10^{-34} J·s, N is the Avogadro's number 6.02252×10^{23} mol^{-1}, R is the universal gas constant, T is the absolute temperature, ΔH_a^* is the enthalpy of activation, and ΔS_a^* is the entropy of activation.

Arrhenius plots of $\text{Log}\,CR$ *versus* $1/T$ of C-steel for blank solution and different concentrations of (BTPTT) were shown in Figure 8. The value of E_a^* can be obtained from the slope $(-E_a^*/R)$ of the straight line (Table 3). It was clear that the values of E_a^* increased with increasing concentration of (BTPTT) and was higher than that in the absence of inhibitor, indicating that the dissolution of C-steel was decreased due to the formation of the high-energy barrier by the adsorption of the inhibitor on the metal surface [37, 38]. The higher E_a^* value in the inhibited solution lead to the lower corrosion rate (CR) and it can be correlated with the increased thickness of the double layer [39]. In this case, the continuous increase in activation energy with the concentration of the inhibitor makes the corrosion process more difficult (higher-energy barrier) which can be ascribed to an increase in thickness of the double layer, giving strong anti-corrosive properties to (BTPTT) and enhancing the electrostatic characteristics of adsorption of the inhibitor on the metal surface (physisorption) [40, 32].

The enthalpy ΔH_a^* and ΔS_a^* of activation values were obtained from the transition state equation (5). A plot of $\text{Log}(CR/T)$ as a function of $1/T$ (Figure 9) was made for C-steel corrosion in 0.1 N HCl in the absence and presence of different concentrations of (BTPTT). Straight lines are obtained with a slope $(-\Delta H_a^*/2.303\,R)$ and intercept $(\text{Log}\,R/Nh + \Delta S_a^*/2.303\,R)$ from which the ΔH_a^* and ΔS_a^* values are calculated (Table 3). In the system, the positive signs of the enthalpies ΔH_a^* indicate the endothermic nature of the C-steel dissolution process. We note that the variation of E_a and ΔH_a^* differ in the same way with the inhibitor's concentration, and this achieves the relationship between E_a and thermodynamics as ΔH_a^*: $E_a^* - \Delta H_a^* = RT$ [41]. The negative sign of ΔS_a^* values either in

the absence or in the presence of the inhibitor (BTPTT) may be explained by the fact that during the formation of the activated complex and in the determining step of the reaction, the reaction is associative rather than dissociative, meaning that a decrease in disorder occurs starting from the reactants to the activated complex [42, 43].

Table 3. Activation parameters for carbon steel in 1 N HCl in absence and presence of different concentrations of BTPTT inhibitor.

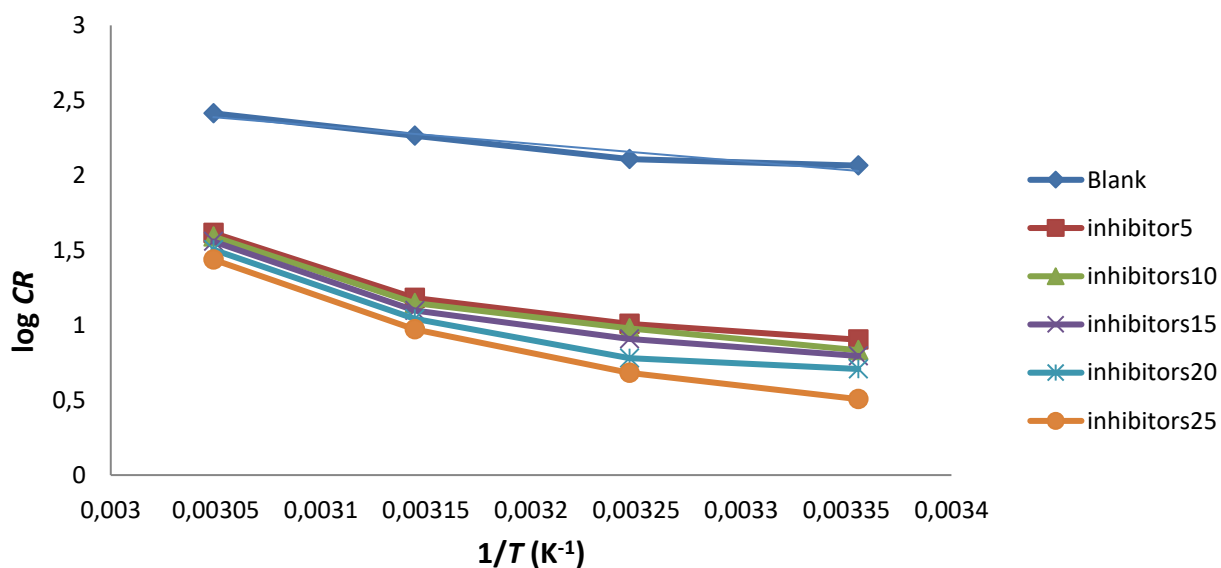| Inhibitor conc. (ppm)	E_a^* (kJ/mol)	ΔH_a^* (kJ/mol)	ΔS_a^* (kJ/mol)	$E_a^* - \Delta H_a^*$ (kJ/mol)
0 (blank)	22.375	19.777	−0.140	2.598
5	42.792	40.194	−0.094	2.598
10	45.394	42.796	−0.087	2.598
15	46.012	43.414	−0.086	2.598
20	49.118	46.520	−0.077	2.598
25	57.367	54.768	−0.053	2.599

Figure 8. Arrhenius plots for the carbon steel in 0.1 N HCl in the absence and presence of different concentrations of BTPTT at different temperatures.
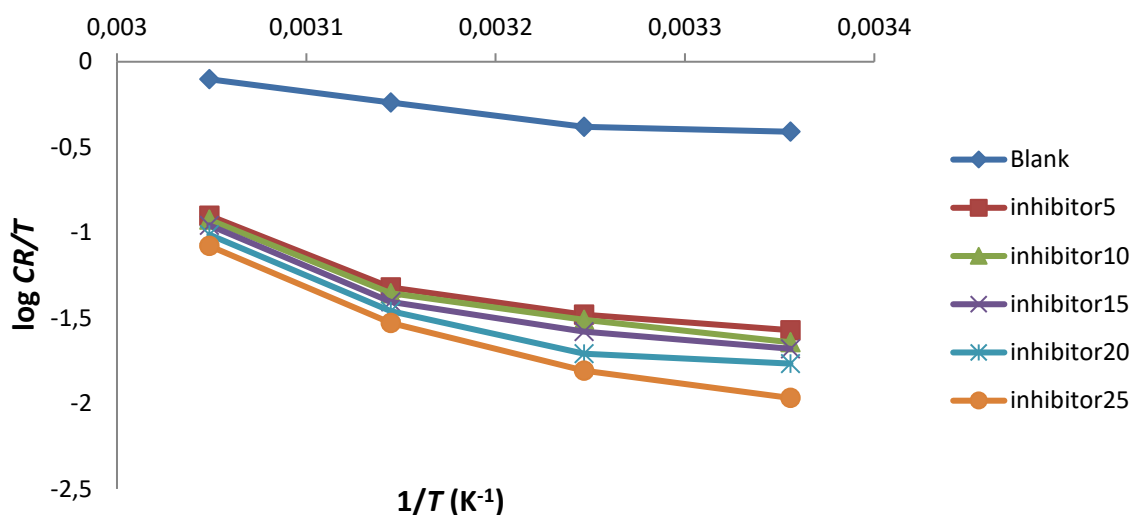
Figure 9. Transition state plots for the carbon steel in 0.1 N HCl in the absence and presence of different concentrations of BTPTT at different temperatures.

3.2. Adsorption isotherm calculations

Calculation of adsorption isotherm is the important method that appear the interaction between the molecules of inhibitor and the metal surface. The degree of surface coverage (θ) obtained from potentiodynamic polarization was utilized to assess the best isotherm that fits into the data obtained. The linear correlation coefficient with R^2 values which is nearer to unity was taken to define the type of adsorption process. According to these results, it can be concluded that the best depiction of the adsorption behavior of BTPTT can be clarified by Langmuir adsorption isotherm which is given by equation (6) [44]:

$$\frac{C}{\theta} = \frac{1}{K_{ads}} + C \tag{6}$$

Where θ is the surface coverage degree, C is the concentration of inhibitor, and K_{ads} is the adsorptive equilibrium constant. The plot of C/θ *versus* C yielded linear graph that is appeared in Figure 10. This explains that the adsorption of the inhibitor molecules on C-steel surface is reliable on Langmuir adsorption isotherm model in various temperatures and the correlation coefficient (R^2) obtained are near to unity. The values of K_{ads} were gotten at various temperatures from the intercepts of the corresponding isotherms. The values of the Gibb's free energy of adsorption (ΔG^0_{ads}) for BTPTT was determined using the following equation [45]:

$$\Delta G^0_{ads} = -RT\ln(55.5 K_{ads}) \tag{7}$$

Where R is the gas constant, T is absolute temperature, and 55.5 is the molar concentration of water in aqueous solution. The values of K_{ads} and ΔG^0_{ads} for the studied inhibitor is reported in Table 4. In the present study, the calculated values of ΔG^0_{ads} of adsorption process were negative and range from -36.499 to -38.647 kJ·mol^{-1} for BTPTT. The negative value of ΔG^0_{ads} indicates that the adsorption of inhibitor on C-steel surface occurs spontaneously. Generally, the values of ΔG^0_{ads} around or less than -20 kJ·mol^{-1} are associated with the electrostatic interaction between charged molecules and the charged metal surface (physisorption); while those around or more negative than -40 kJ·mol^{-1} involves sharing or transfer of electrons from the inhibitor molecules to the metal surface to form a coordinate type of metal bond (chemisorption) [26, 29, 33].
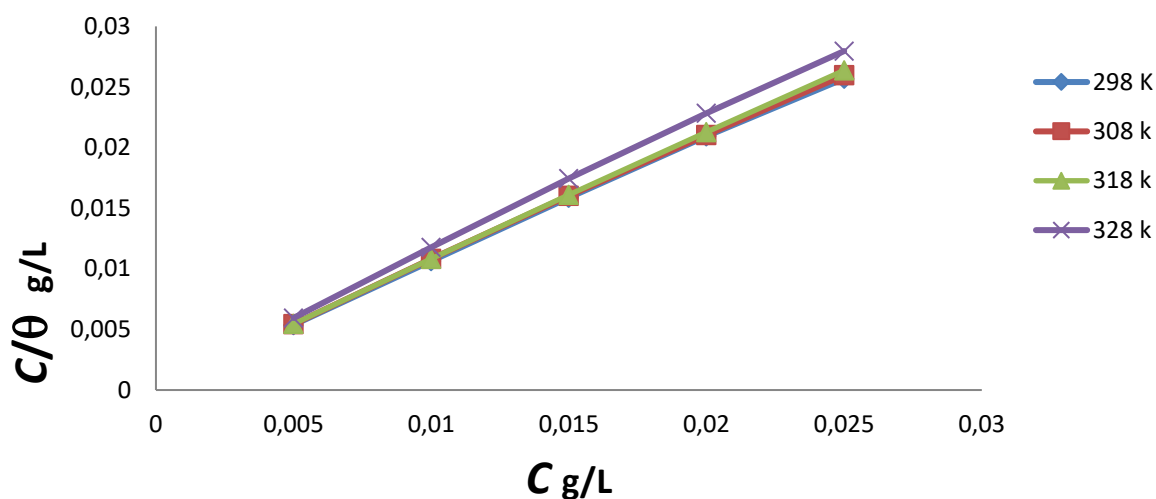

Figure 10. Langmuir isotherm for the adsorption of BTPTT on the surface of carbon steel in 0.1 M HCl.

Table 4. Adsorption parameters for adsorption BTPTT on carbon steel surface in 0.1 N HCl solution at different temperatures.

Inhibitor	T (K)	R^2	K_{ads} (L·mol^{-1})	ΔG^0_{ads} (kJ·mol^{-1})
BTPTT	298	0.9996	2500	−36.499
	308	0.9997	2000	−37.153
	318	0.9999	3333.333	−39.710
	328	0.9993	1428.571	−38.648

In the case of BTPTT, ΔG^0_{ads} value of the inhibitor was found to be from -36.499 to -38.647 kJ·mol^{-1}, this indicates the phenomena of the adsorption mechanism of inhibitor on C-steel surface in 0.1 N HCl solution was typical of chemisorption. This may be credited to the strong adsorption of inhibitor molecules on C-steel surface due to the presence of the free electron pairs on S and O atoms as well as π-electrons of the aromatic rings [46]. The heteroatoms (S), (O) and π-electrons of the organic compounds act as the reaction sites in adsorption process [29]. The adsorption of inhibitor molecules on C-steel surface can be interpreted on the ground of electrostatic and/or donor acceptor interaction between electron density of S, O and aromatic rings of inhibitor and vacant d-orbitals of iron atoms at the surface [44].

3.3. Thermal analysis TGA and DTA for inhibitor BTPTT

Figure 11 which show the thermal analysis curve TGA and DTA of (BTPTT). From the curve the inhibitor was thermally stable up to temperature 150°C and the T_{max} (temperature of decomposition) was 221.25°C. The estimated difference between the two thermal degrees ΔT is 128°C.
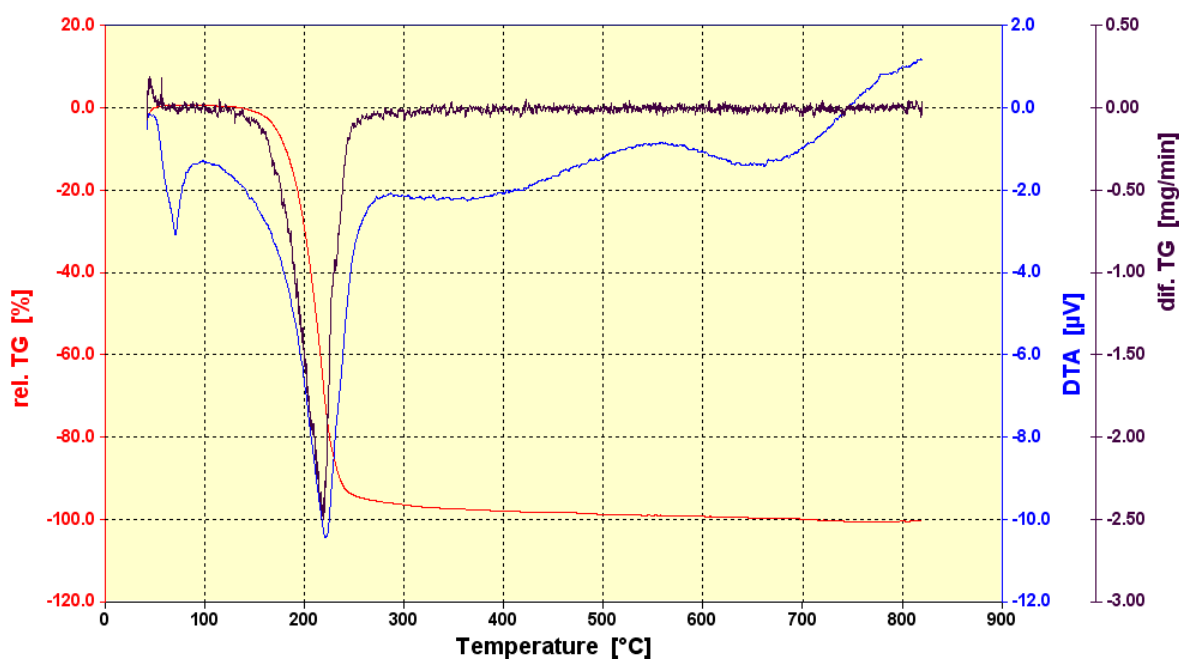

Figure 11. The thermal analysis, TGA and DTA of BTPTT inhibitor.

Table 5. The functions of thermal analysis (TGA and DTA) of BTPTT.

Decomposition temperature (T_{max})	221.25°C
50 wt% loss ($T1/2$)	205°C
$\Delta T = T_f - T_i = (300 - 172)$°C	128°C

4. Conclusion

Bis(3-mercaptopropyl)thioterephthalate (BTPTT) presents good effectiveness in 0.1 N HCl and even at higher temperature. The inhibition efficiency increments with rise of concentration and diminishes with temperature. The adsorption of the prepared compound follows the Langmuir's adsorption. The inhibitor adsorption on the C-steel surface is chemically adsorbed, while the negative values of ΔG_{ads} show the spontaneity of the adsorption process.

References

1. S.M. Al-Salem, P. Lettieri and J. Baeyens, Recycling and Recovery Routes of Plastic Solid Waste (PSW): A review, *Waste Manage.*, 2009, **29**, no. 10, 2625–2643. doi: 10.1016/j.wasman.2009.06.004

2. T. Chilton, S. Burnley and S. Nesaratnam, A Life Cycle Assessment of the Closed-Loop Recycling and Thermal Recovery of Post-Consumer PET, *Resour., Conserv. Recycl.*, 2010, **54**, no. 12, 1241–1249. doi: 10.1016/j.resconrec.2010.04.002

3. A.P. Siroèiæ, A. Fijaèko and Z. Hrnjak-Murgiæ, Chemical Recycling of Postconsumer Poly(ethylene-terephthalate) Bottles – Depolymerization Study, *Chem. Biochem. Eng. Q.*, 2013, **27**, no. 1, 65–71.

4. A. Archna, V. Moses, S. Sagar, V. Shivraj and S. Chetan, A Review on Processing of Waste PET (Polyethylene Terephthalate) Plastics, *Int. J. Polym. Sci. Eng.*, 2015, **1**, no. 2, 1–13.

5. F. Awaja and D. Pavel, Recycling of PET, *Eur. Polym. J.*, 2005, **41**, 1453–1477.

6. A.H. Yasir, A.S. Khalaf and M.N. Khalaf, Preparation and Characterization of Oligomer from Recycled PET and Evaluated as a Corrosion Inhibitor for C-Steel Material in 0.1 M HCl, *Open J. Org. Polym. Mater.*, 2017, **7**, no. 1, 1–15. doi: 10.4236/ojopm.2017.71001

7. B.D.B. Tiu and R.C. Advincula, Polymeric corrosion inhibitors for the oil and gas industry: Design principles and mechanism, *React. Funct. Polym.*, 2015, **95**, 25–45. doi: 10.1016/j.reactfunctpolym.2015.08.006

8. Y.P. Lolage, P.R. Pawar, V.B. Yannawar and A.B. Bhosle, Corrosion Studies Of Selected Metals From Industrial Effluent In Pune Midc, India, *BMC Health Serv. Res.*, 2013, **3**, no. 3, 1–3.

9. M. Valipour, M. Shekarchi and P. Ghods, Comparative Studies of Experimental and Numerical Techniques in Measurement of Corrosion Rate and Time-to-Corrosion-Initiation of Rebar in Concrete in Marine Environments, *Cem. Concr. Compos.*, 2014, **48**, 98–107. doi: 10.1016/j.cemconcomp.2013.11.001

10. W. Wu, Z. Liu and D. Krys, Improving Laser Image Resolution for Pitting Corrosion Measurement Using Markov Random Field Method, *Autom. Constr.*, 2012, **21**, 172–183. doi: 10.1016/j.autcon.2011.06.002

11. A. Alvarez-Pampliega, T. Hauffman, M. Petrova, T. Breugelmansa, T. Muselle, K. Van den Bergh, J. De Strycker, H. Terryn and A. Hubin, Corrosion Study on Al-Rich Metal-Coated Steel by Odd Random Phase Multisine Electrochemical Impedance Spectroscopy, *Electrochim. Acta*, 2014, **124**, 165–175. doi: 10.1016/j.electacta.2013.09.159

12. D.K. Yadav, B. Maiti and M.A. Quraishi, Electrochemical and quantum chemical studies of 3,4-dihydropyrimidin-2(1*H*)-ones as corrosion inhibitors for mild steel in hydrochloric acid solution, *Corros. Sci.*, 2010, **52**, no. 11, 3586–3598. doi: 10.1016/j.corsci.2010.06.030

13. S.N. Roselli, G. Lendvay-Györik, G. Mészáros, C. Deyá and R. Romagnoli, Anticorrosive water borne paints free from zinc and with reduced phosphate content, *Prog. Org. Coat.*, 2017, **112**, 27–36. doi: 10.1016/j.porgcoat.2017.04.023

14. G. khan, K.S. Newaz, W.J. Basirun, H.B.M. Ali, F.L. Faraj and G.M. Khan, Application of natural product extracts as green corrosion inhibitors for metals and alloys in acid pickling processes – A review, *Int. J. Electrochem. Sci.*, 2015, **10**, no. 8, 6120–6134.

15. G. Sığırcık, T. Tüken and M. Erbil, Assessment of the inhibition efficiency of 3,4-diaminobenzonitrile against the corrosion of steel, *Corros. Sci.*, 2016, **102**, 437–445. doi: 10.1016/j.corsci.2015.10.036

16. Ali A. Naser, Alaa S. Al-Mubarak and Hazi Z. Al-Sawaad, Synthesis, characterization and evaluation of some graphene oxide derivatives and their application as corrosion inhibitors for carbon steel alloy type C1025 in hydrochloric acid, *Int. J. Corros. Scale Inhib.*, 2019, **8**, no. 4, 974–997. doi: 10.17675/2305-6894-2019-8-4-11

17. H. Keleş, D.M. Emir and M. Keleş, A comparative study of the corrosion inhibition of low carbon steel in HCl solution by an imine compound and its cobalt complex, *Corros. Sci.*, 2015, **101**, 19–31. doi: 10.1016/j.corsci.2015.07.013

18. A.M. Al-Sabagh, F.Z. Yehia, Gh. Eshaq, A.M. Rabie and A.E. El Metwally, Greener routes for recycling of polyethylene terephthalate, *Egypt. J. Pet.*, 2016, **25**, no. 1, 53–64. doi: 10.1016/j.ejpe.2015.03.001

19. R.S. Abd El-Hameed, Aminolysis of Polyethylene Terephthalate Waste as Corrosion Inhibitor for Carbon Steel in HCl Corrosive Medium, *Adv. Appl. Sci. Res.*, 2011, **2**, no. 3, 483–499.

20. L.A. Al Juhaiman, Polyvinyl Pyrrolidone as a Corrosion Inhibitor for Carbon Steel in HCl, *Int. J. Electrochem. Sci.*, 2016, **11**, 2247–2262.

21. A. Kadhim, A.K. Al-Okbi, D.M. Jamil, A. Qussay, A.A. Al-Amiery, T.S. Gaaz, A.H. Kadhum, A.B. Mohamad and M.H. Nassir, Experimental and theoretical studies of benzoxazines corrosion inhibitors, *Results Phys.*, 2017, **7**, 4013–4019. doi: 10.1016/j.rinp.2017.10.027

22. M.A. Chidiebere, E.E. Oguzie, L. Liu, Y.P. Li and F. Wang, Adsorption and corrosion inhibiting effect of riboflavin on Q235 mild steel corrosion in acidic environments, *Mater. Chem. Phys.*, 2015, **156**, 95–104. doi: 10.1016/j.matchemphys.2015.02.031

23. H. Ashassi-Sorkhabi, B. Shaabani and D. Seifzadeh, Corrosion inhibition of mild steel by some Schiff base compounds in hydrochloric acid, *Appl. Surf. Sci.*, 2005, **239**, no. 2, 154–164. doi: 10.1016/j.apsusc.2004.05.143

24. S. Martinez and I. Stern, Thermodynamic characterization of metal dissolution and inhibitor adsorption processes in the low carbon steel/mimosa tannin/sulfuric acid system, *Appl. Surf. Sci.*, 2002, **199**, no. 1–4, 83–89. doi: [10.1016/S0169-4332(02)00546-9](10.1016/S0169-4332(02)00546-9)

25. F. Mohsenifar, H. Jafari and K. Sayin, Investigation of Thermodynamic Parameters for Steel Corrosion in Acidic Solution in the Presence of N,N′-Bis(phloroacetophenone)-1,2 propanediamine, *J. Bio- Tribo-Corros.*, 2016, **2**, no. 1, 1–13. doi: [10.1007/s40735-015-0031-y](10.1007/s40735-015-0031-y)

26. M.H. Mahross, A.H. Naggar, T.A.S. Elnasr and M. Abdel-Hakim, Effect of Rice Straw Extract as an Environmental Waste Corrosion Inhibitor on Mild Steel in an Acidic Media, *Chem. Adv. Mater.*, 2016, **1**, no. 1, 6–16.

27. T. Zakroczymski and J. Flis, Impedance characterization of the activation of iron surface for hydrogen entry from alkaline solution, *Electrochim. Acta*, 1996, **41**, no. 7–8, 1245–1250. doi: [10.1016/0013-4686(95)00477-7](10.1016/0013-4686(95)00477-7)

28. E. Khamis, F. Bellucci, R.M. Latanision and E.S.H. El-Ashry, Acid Corrosion Inhibition of Nickel by 2-(Triphenosphoranylidene) Succinic Anhydride, *Corrosion*, 1991, **47**, no. 9, 677–686. doi: [10.5006/1.3585307](10.5006/1.3585307)

29. S.A.X. Stangu and U. Vijayalakshmi, Studies on corrosion inhibitory effect and adsorption behavior of waste materials on mild steel in acidic medium, *J. Asian Ceram. Soc.*, 2018, **6**, no. 1, 20–29. doi: [10.1080/21870764.2018.1439608](10.1080/21870764.2018.1439608)

30. T. Ramdé, S. Rossi and C. Zanella, Inhibition of the Cu65/Zn35 brass corrosion by natural extract of *Camellia sinensis*, *Appl. Surf. Sci.*, 2014, **307**, 209–216. doi: 10.1016/j.apsusc.2014.04.016

31. C.B. Pradeep Kumar, K.N. Mohana and H.B. Muralidhara, Electrochemical and thermodynamic studies to evaluate the inhibition effect of synthesized piperidine derivatives on the corrosion of mild steel in acidic medium, *Ionics*, 2015, **21**, no. 1, 263–281. doi: [10.1007/s11581-014-1178-0](10.1007/s11581-014-1178-0)

32. A. Fiala, W. Boukhedena, S. Lemallem, H. Ladouani and H. Allal, Inhibition of Carbon Steel Corrosion in HCl and H_2SO_4 Solutions by Ethyl 2-Cyano-2-(1,3-dithian-2-ylidene) Acetate, *J. Bio- Tribo-Corros.*, 2019, **5**, no. 2, 42. doi: [10.1007/s40735-019-0237-5](10.1007/s40735-019-0237-5)

33. H.J. Habeeb, H.M. Luaibi, R.M. Dakhil, A.H. Kadhum, A.A. Al-Amiery and T.S. Gaaz, Development of new corrosion inhibitor tested on mild steel supported by electrochemical study, *Results Phys.*, 2018, **8**, 1260–1267. doi: 10.1016/j.rinp.2018.02.015

34. A.K. Singh, A.K. Singh and E.E. Ebenso, Inhibition Effect of Cefradine on Corrosion of Mild Steel in HCl Solution, *Int. J. Electrochem. Sci.*, 2014, **9**, no. 1, 352–364.

35. B. Zerga, B. Hammouti, M. Touhami, R. Touir, M. Taleb, M. Sfaira, M. Bennajeh and I. Forssal, Comparative Inhibition Study of New Synthesised Pyridazine Derivatives towards Mild Steel Corrosion in Hydrochloric Acid. Part-II: Thermodynamic Proprieties, *Int. J. Electrochem. Sci.*, 2012, **7**, no. 1, 471–483.

36. J. Bhat and V. Alva, Corrosion Inhibition of Aluminium by 2-Chloronicotinic Acid in HCl Medium, *Indian J. Chem. Technol.*, 2009, **16**, 228–233.

37. R. Solmaz, G. Kardaş, B. Yazıcı and M. Erbil, Adsorption and Corrosion Inhibitive Properties of 2-Amino-5-Mercapto-1,3,4-Thiadiazole on Mild Steel in Hydrochloric Acid Media, *Colloids Surf., A*, 2008, **312**, no. 1, 7–17. doi: 10.1016/j.colsurfa.2007.06.035

38. M.H. Hussin and M.J. Kassim, The corrosion inhibition and adsorption behavior of *Uncaria gambir* extract on mild steel in 1 M HCl, *Mater. Chem. Phys.*, 2011, **125**, no. 3, 461–468. doi: 10.1016/j.matchemphys.2010.10.032

39. M.R. Singh, K. Bhrara and G. Singh, The inhibitory effect of diethanolamine on corrosion of mild steel in 0.5 M sulphuric acidic medium, *Port. Electrochim. Acta*, 2008, **26**, no. 6, 479–492. doi: 10.4152/pea.200806479

40. I.B. Obot and N.O. Obi-Egbedi, Inhibitory effect and adsorption characteristics of 2,3-diaminonaphthalene at aluminum/hydrochloric acid interface: experimental and theoretical study, *Surf. Rev. Lett.*, 2008, **15**, no. 6, 903–910. doi: 10.1142/S0218625X08012074

41. G.K. Gomma and M.H. Wahdan, Schiff bases as corrosion inhibitors for aluminium in hydrochloric acid solution, *Mater. Chem. Phys.*, 1995, **39**, no. 3, 209–213. doi: 10.1016/0254-0584(94)01436-K

42. A.M. Al-Fakih, M. Aziz and H.M. Sirat, Turmeric and ginger as green inhibitors of mild steel corrosion in acidic medium, *J. Mater. Environ. Sci.*, 2015, **6**, no. 5, 1480–1487.

43. A.S. Fouda, A.A. Al-Sarawy and E.E. El-Katori, Pyrazolone derivatives as corrosion inhibitors for C-steel in hydrochloric acid solution, *Desalination*, 2006, **201**, no. 1–3, 1–13. doi: 10.1016/j.desal.2006.03.519

44. I. Ahamad and M.A. Quraishi, Bis (benzimidazol-2-yl) disulphide: an efficient water soluble inhibitor for corrosion of mild steel in acid media, *Corros. Sci.*, **51**, no. 9, 2006–2013. doi: 10.1016/j.corsci.2009.05.026

45. P. Singh and M.A. Quraishi, Corrosion inhibition of mild steel using Novel Bis Schiff's Bases as corrosion inhibitors: Electrochemical and Surface measurement, *Measurement*, 2016, **86**, 114–124. doi: 10.1016/j.measurement.2016.02.052

46. M. Erna, H. Herdini and D. Futra, Corrosion Inhibition Mechanism of Mild Steel by Amylose-Acetate/Carboxymethyl Chitosan Composites in Acidic Media, *Int. J. Chem. Eng.*, 2019, 8514132. doi: 10.1155/2019/8514132

♦ ♦ ♦